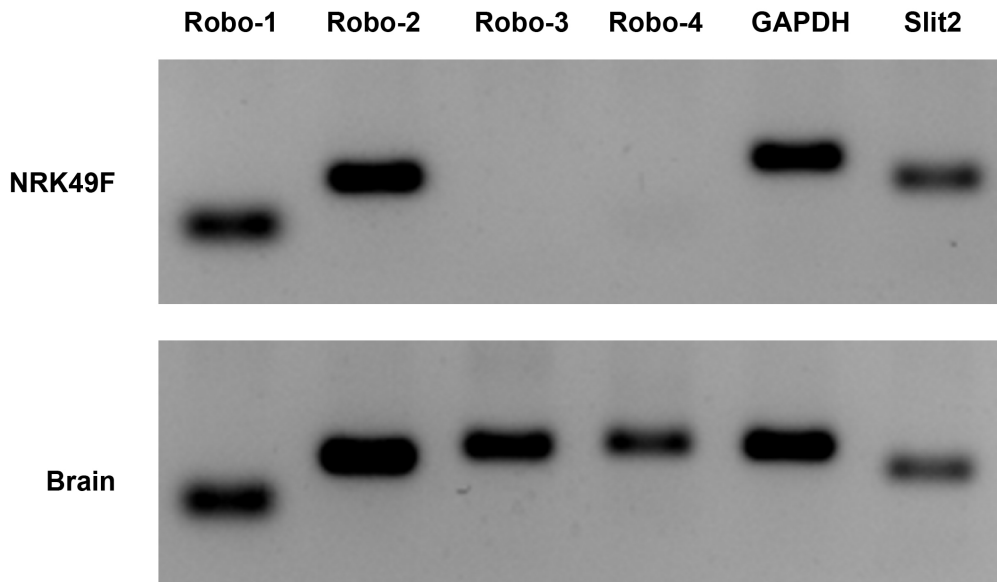


## SUPPLEMENTAL INFORMATION

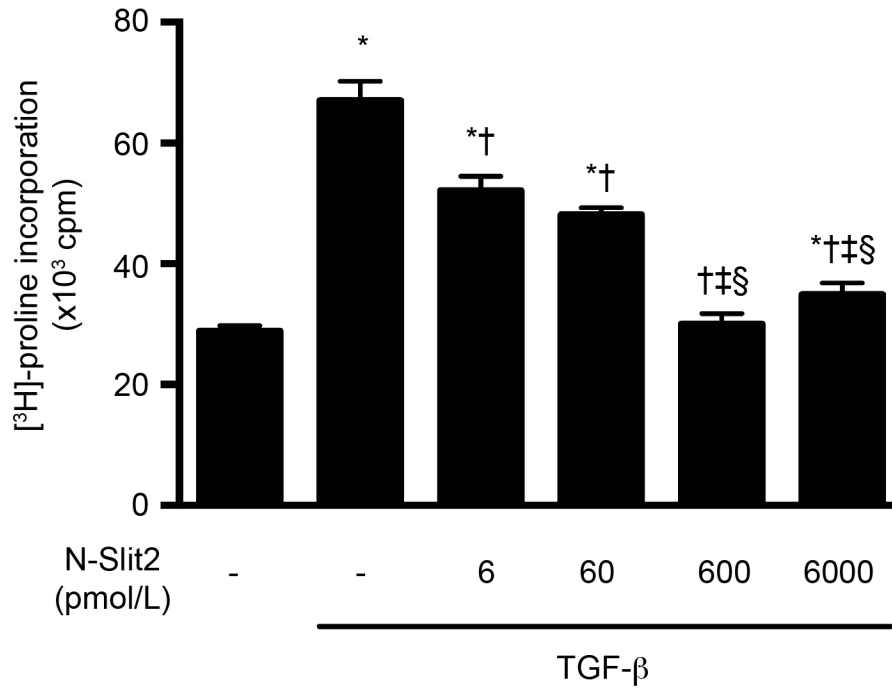
### Supplemental Figure 1



**Supplemental Figure 1: NRK49F renal fibroblasts express detectable mRNA levels of Slit2, Robo-1, and Robo-2, but not Robo-3 or Robo-4.**

Expression of Slit2 and its Robo receptors was assessed in NRK49F fibroblasts using RT-PCR. Rat brain was used as a positive control.

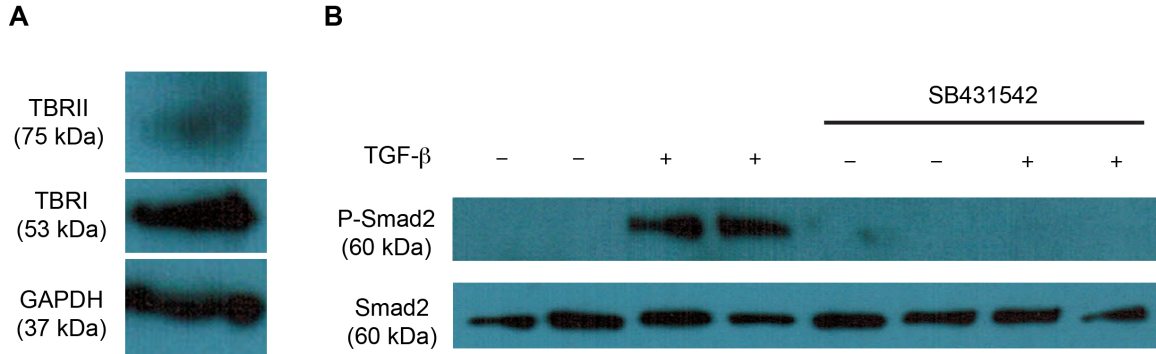
## Supplemental Figure 2



### Supplemental Figure 2: Slit2 inhibits TGF- $\beta$ -induced collagen production even when given after TGF- $\beta$ stimulation.

NRK49F fibroblasts were incubated with TGF- $\beta$  (10 ng/mL), and 4 hours later, N-Slit2 was added at the indicated concentrations. Incorporation of [<sup>3</sup>H]-proline into protein, a marker of collagen production, was measured. n = 3. \* p < 0.05 vs. control. † p < 0.05 vs. TGF- $\beta$ -stimulated cells. ‡ p < 0.05 vs. TGF- $\beta$ - and N-Slit2 (6 pmol/L)-treated cells. § p < 0.05 vs. TGF- $\beta$ - and N-Slit2 (60 pmol/L)-treated cells.

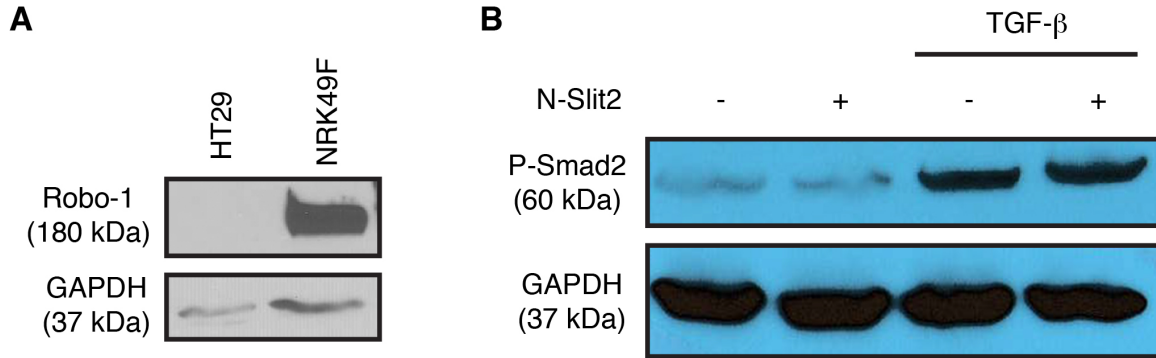
### Supplemental Figure 3



**Supplemental Figure 3: NRK49F renal fibroblasts express components of the TGF- $\beta$  receptor complex and mount a robust Smad2 phosphorylation response to TGF- $\beta$ .**

(A) NRK49F renal fibroblast cell lysates were probed with antibodies directed against GAPDH and the TGF- $\beta$  receptor type 1 (TBR1) and 2 (TBR2). (B) NRK49F fibroblasts were pre-treated with or without the TBR1 inhibitor SB431542 100  $\mu$ mol/L for 1 hr, then stimulated with or without TGF- $\beta$  10 ng/mL for 30 mins. Cell lysates were then probed with antibodies directed against C-terminally phosphorylated Smad2 or total Smad2/3. The blots shown are representative of  $n = 3$  independent experiments.

## Supplemental Figure 4

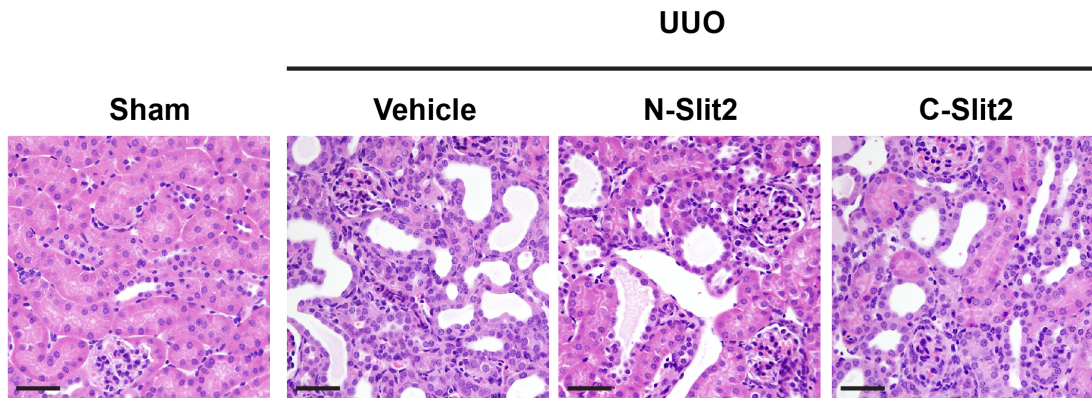


**Supplemental Figure 4: In HT29 cells, which do not express Robo-1, N-Slit2 does not inhibit Smad2 phosphorylation induced by TGF- $\beta$ .**

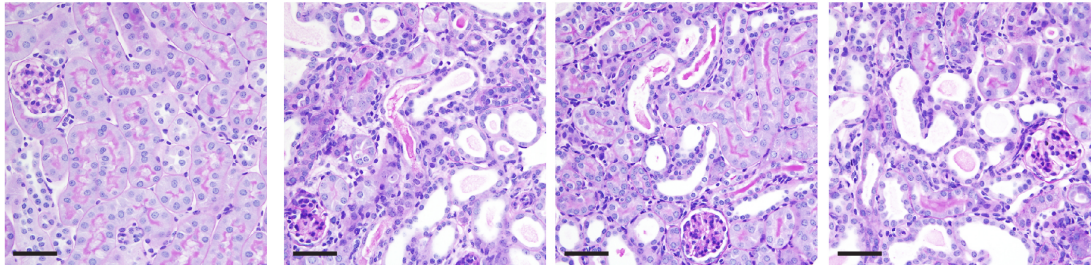
(A) HT29 epithelial cells and NRK49F renal fibroblasts were lysed, and lysates were immunoblotted for Robo-1 and GAPDH. (B) Following overnight serum starvation, HT29 epithelial cells were incubated with or without N-Slit2 (30 nmol/L) for 10 min and/or TGF- $\beta$  10 ng/mL for 30 min. Cells were lysed, and lysates were immunoblotted for phosphorylated Smad2 (P-Smad2) and GAPDH. A blot representative of three replicates is shown.

## Supplemental Figure 5

A



B

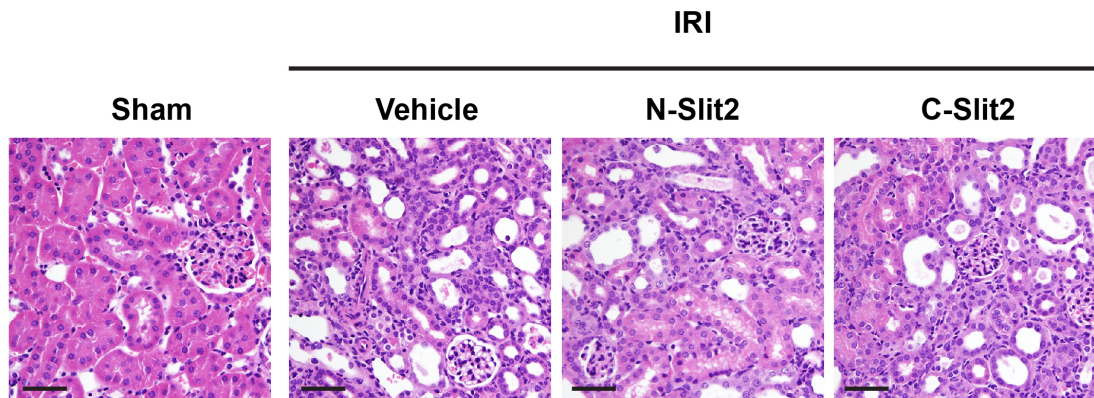


**Supplemental Figure 5: Following Uuo, injured kidneys developed significant tubular injury and inflammation.**

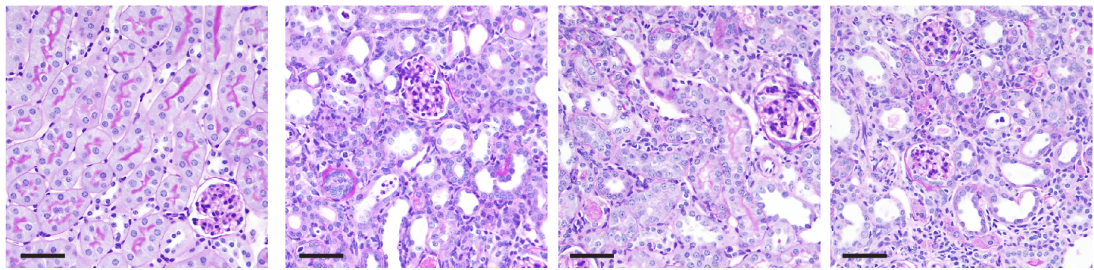
Mice were subjected to Uuo and control vehicle (n = 18), N-Slit2 (n = 12), or C-Slit2 (n = 12) administered as described in the complete “Methods” section (Supplemental Information). Sham-operated mice (n = 12) served as controls. After 7 d, mice were sacrificed and kidney sections stained with (A) hematoxylin and eosin, and (B) Periodic Acid-Schiff stains. Representative images were taken with a 20X objective. Scale bar = 50  $\mu$ m.

## Supplemental Figure 6

A



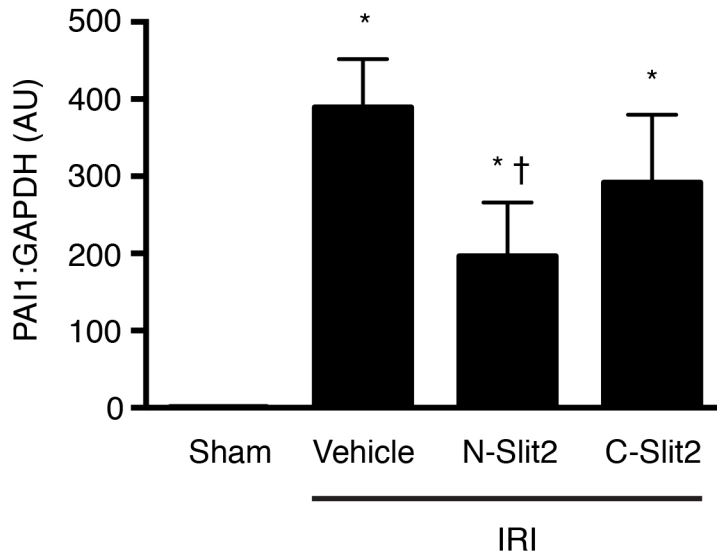
B



**Supplemental Figure 6: Following IRI, injured kidneys developed significant tubular injury and inflammation.**

Mice were subjected to renal IRI, and control vehicle (n = 17), N-Slit2 (n = 17), or C-Slit2 (n = 7) administered as described in the complete “Methods” section (Supplemental Information). Sham-operated mice (n = 6) served as controls. After 14 d, mice were sacrificed and kidney sections stained with (A) hematoxylin and eosin, and (B) Periodic Acid-Schiff stains. Representative images were taken with a 20X objective. Scale bar = 50  $\mu$ m.

### Supplemental Figure 7

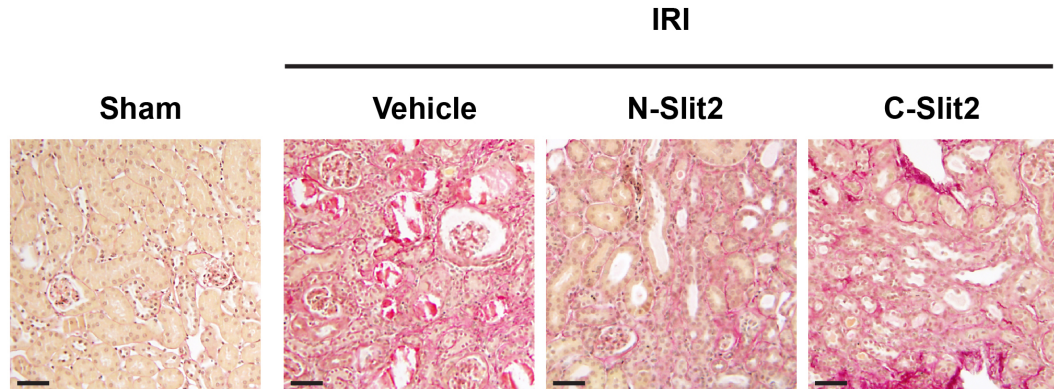


### Supplemental Figure 7: N-Slit2 treatment attenuates PAI1 expression induced by unilateral ischemia-reperfusion injury (IRI).

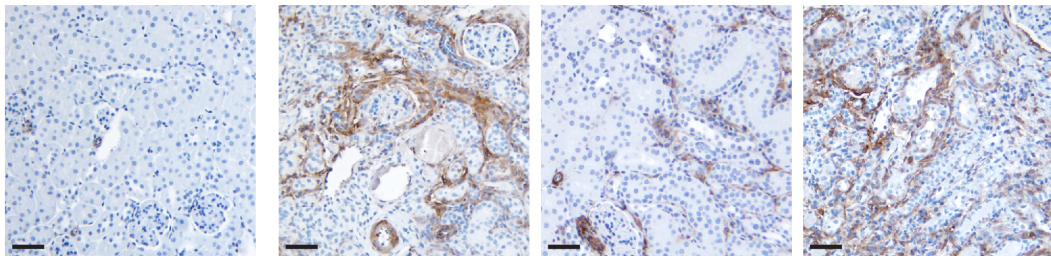
Mice were subjected to renal IRI, and control vehicle (n = 17), N-Slit2 (n = 17), or C-Slit2 (n = 7) administered as described in the complete “Methods” section (Supplemental Information). Sham-operated mice (n = 6) served as controls. Following kidney resection at study end, RNA was isolated from kidney homogenates, reverse transcribed and qPCR performed to measure the relative levels of PAI1 between the four treatment groups. \* p < 0.05 vs. sham controls. † p < 0.05 vs vehicle.

## Supplemental Figure 8

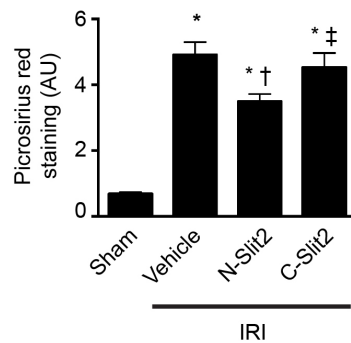
A



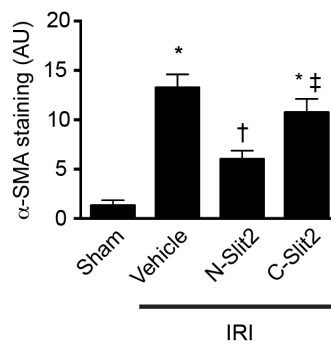
B



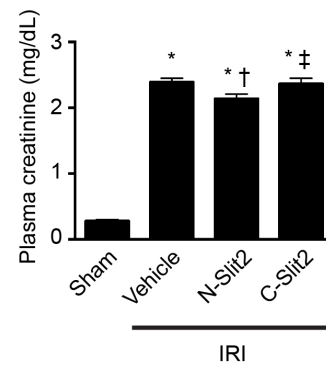
C



D



E



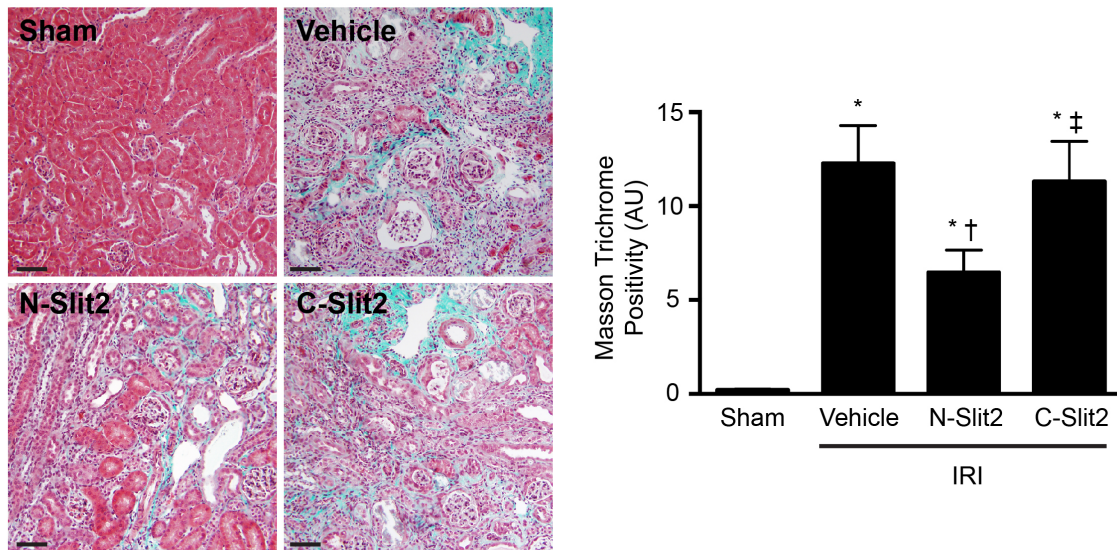
**Supplemental Figure 8: Slit2 treatment reduces fibrosis and kidney dysfunction following ischemia-reperfusion injury (IRI), even when administered 72 h post-insult.**

Mice were subjected to renal IRI, and control vehicle (n = 15), N-Slit2 (n = 15), or C-Slit2 (n = 14) as described in the “Methods” section (Supplemental Information). Sham-operated mice (n = 3) served as controls. Mice given N-Slit2 or C-Slit2 received their

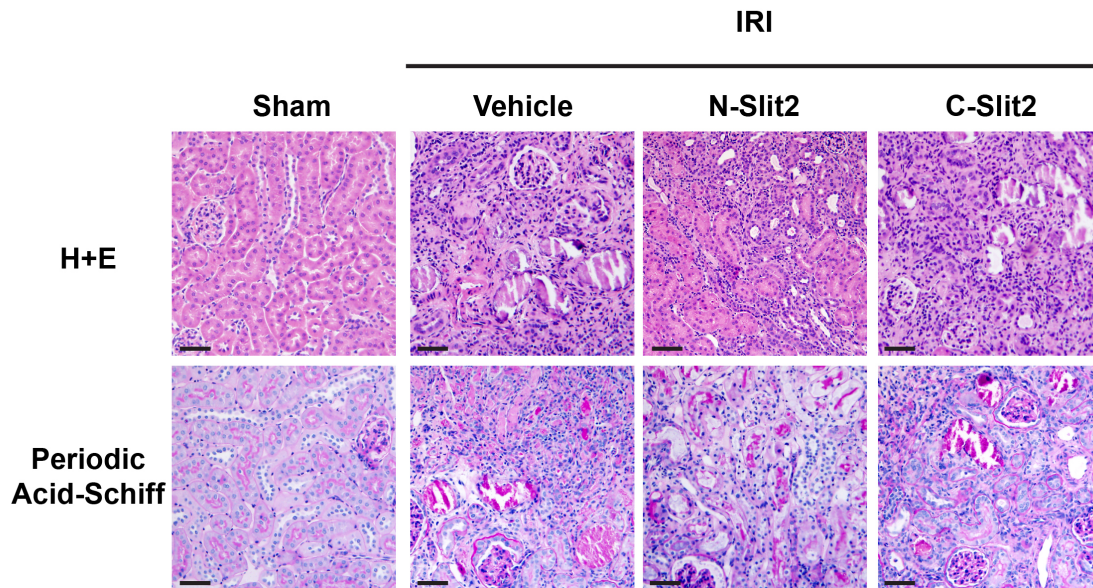
first injections 72 h after surgery. Fourteen days after surgery, mice were sacrificed and kidney sections labeled with picosirius red (PSR) to detect fibrillar collagen (A), or with antibody directed to  $\alpha$ -smooth muscle actin ( $\alpha$ -SMA) (B). Representative images (20X objective); scale bar: 50  $\mu$ m. (C) Experiments were performed as in (A) and PSR labeling digitally quantified. (D) Experiments were performed as in (B) and  $\alpha$ -SMA labeling digitally quantified. One day prior to sacrifice, all animals underwent nephrectomy to remove the uninjured right kidney. (E) The next day, blood was collected for measurement of plasma creatinine. Mean values  $\pm$  SEM. \*  $p < 0.05$  vs. sham controls. †  $p < 0.05$  vs. vehicle. ‡  $p < 0.05$  vs. N-Slit2. AU, arbitrary units. One-way ANOVA with post-hoc Fisher's least significant difference was performed.

## Supplemental Figure 9

A



B



**Supplemental Figure 9: Slit2 administration reduces extracellular matrix deposition even when administered beginning 72 h post-ischemia-reperfusion injury (IRI).**

Mice were subjected to renal IRI, and control vehicle (n = 15), N-Slit2 (n = 15), or C-Slit2 (n = 14) administered as described in the complete “Methods” section (Supplemental Information). Sham-operated mice (n = 3) served as controls. (A) After

14 d, mice were sacrificed and kidney sections stained with Masson's Trichrome and deposited extracellular matrix digitally quantified. Kidney sections were also stained with (B) hematoxylin and eosin (H+E) and Periodic Acid-Schiff stains, demonstrating significant tubular injury in all treatment groups. Mean values  $\pm$  SEM. \*  $p < 0.05$  vs. sham controls. †  $p < 0.05$  vs. vehicle. ‡  $p < 0.05$  vs. N-Slit2. AU, arbitrary units. One-way ANOVA with post-hoc Fisher's least significant difference was performed. All images were taken with a 20X objective. Scale bar = 50  $\mu$ m.

## **COMPLETE METHODS**

### **Slit2 and Robo-N expression and purification**

A bio-active N-terminal fragment of human Slit2 (N-Slit2) and the soluble Slit2 decoy receptor, Robo-N, were generated as previously described <sup>1-3</sup>. A bio-inactive truncated C-terminal fragment of Slit2 (C-Slit2) was produced by subcloning a cDNA encoding a peptide corresponding to the T1268-S1525 residues of Slit2 downstream of 6 tandem His tags, followed by transient transfection into HEK293-6E cells and Fractogel-cobalt column purification of conditioned medium as previously described <sup>1-3</sup>.

### **Cell culture**

Immortalized normal rat kidney interstitial fibroblasts (NRK49F) were purchased from ATCC. DLD-1 colon cancer epithelial cells were a kind gift of Dr. Ming Tsao, while HT29 colon cancer epithelial cells were purchased from ATCC (Manassas, VA). Both epithelial cell lines have been reported to lack Robo-1 <sup>4</sup>. Cells were cultured at 37°C with 5% CO<sub>2</sub> and grown in Dulbecco's Modified Eagle Medium supplemented with 5% or 10% Fetal Bovine Serum (Life Technologies, Burlington, Canada).

### **Detection of Robo-1 in cultured fibroblasts**

mRNA levels of Slit2 and its Robo receptors were assessed using reverse-transcription-PCR (RT-PCR). Total RNA was isolated using one-step RNA reagent (BIO BASIC INC, Unionville, Canada). RT-PCR was then performed using a One-Step RT-PCR Kit (QIAGEN, Toronto, Canada) as per the manufacturer's instructions. The following sequence-specific primers were used: (1) Robo-1 Forward:

ATGACTGCTCCATCAACTGCTGCACA,	and	Robo-1	Reverse:
TGCTATAACAATCAGCTGGGCGACT,	(2)	Robo-2	Forward:
ACCAACATTCAGCGTTCAGATGCG	and	Robo-2	Reverse:
GCCATCTACCGCAAGTGTTTGGTT,	(3)	Robo-3	Forward:
ATGTGAGACCAAAGGAAACCCACCA	and	Robo-3	Reverse:
ACTGACAGCCTGGCACACATAGTA,	(4)	Robo-4	Forward:
TCTGTTCCCCACGCATGTCTCT	and	Robo-4	Reverse:
TCTCGTGGGGAACAAGTGTTTG,	(5)	Slit2	Forward:
TTTGCCTGGCTACTTGGGAGAGAA	and	Slit2	Reverse:
TGTACAAGAGGATGCCGCTGTCTT;	and (6)	GAPDH	Forward:
AAGATGGTGAAGGTCGGTGTG	and	GAPDH	Reverse:

TTCCATTCTCAGCCTTGAC. Rat brain tissue homogenate served as a positive control, and a no template reaction served as a negative control. PCR products were separated by 1.5% agarose gel electrophoresis. Robo-1 protein was examined using immunoblotting and immunofluorescence staining. For immunoblotting, NRK49F, DLD-1, HT29, or rat brain lysates were probed with a rabbit anti-Robo-1 antibody (Ab) directed against the intracellular domain of Robo-1 (Rockland Immunochemicals, Gilbertsville, PA), and detected using a horseradish peroxidase (HRP)-conjugated goat anti-rabbit secondary Ab (Jackson ImmunoResearch, West Grove, PA). For immunofluorescence staining, NRK49F cells grown on glass coverslips were labeled with anti-Robo-1 Ab followed by an Alexa488-conjugated donkey anti-rabbit secondary Ab (Jackson ImmunoResearch). Cells were counter-stained with DAPI to identify nuclei and imaged at room temperature using the Volocity imaging package (PerkinElmer,

Waltham, MA) on a spinning disc DMIRE2 confocal microscope (Leica Microsystems, Toronto, Canada) equipped with a Hamamatsu digital camera <sup>1-3</sup>.

### **[<sup>3</sup>H]-proline incorporation assay**

Following serum starvation, NRK49F cells were incubated with varying concentrations of N-Slit2 for 10 min, followed by transforming growth factor- $\beta$  (TGF- $\beta$ ; 10 ng/ml; R & D Systems, Minneapolis, MN), and [<sup>3</sup>H]-proline (1  $\mu$ Ci/well, GE Healthcare, Baie d'Urfe, Canada) for 44 h. Alternately, [<sup>3</sup>H]-proline incorporation was also measured when NRK49F cells were stimulated with TGF- $\beta$  for 4 hrs prior to administration of N-Slit2. In separate experiments, NRK49F cells were incubated with N-Slit2 30 nmol/L pre-mixed with molar equivalent amounts of Robo-N <sup>5</sup>. Protein was acid precipitated, and following washing to remove unincorporated [<sup>3</sup>H]-proline, the amount of [<sup>3</sup>H]-proline incorporated was measured using a liquid scintillation counter as a sensitive measure of collagen production (LS 6000 Beckman Instruments, Beckman Coulter, Mississauga, Canada) <sup>6-9</sup>.

### **Imaging of actin stress fiber formation**

NRK49F cells were incubated with N-Slit2 (60 nmol/l) for 30 min, followed by TGF- $\beta$  (10 ng/ml) for 30 min. Cells were fixed, permeabilized and labeled with Alexa488-conjugated phalloidin (Life Technologies, Burlington, Canada) to visualize polymerized filamentous actin (F-actin), and counterstained with DAPI to identify nuclei. Cells were examined at room temperature using the Volocity imaging package (PerkinElmer) on a spinning disc DMIRE2 confocal microscope (Leica Microsystems) equipped with a

Hamamatsu digital camera <sup>2</sup>. Total actin stress fiber length per cell was calculated by measuring the total length of non-cortical actin stress fibers in all cells in 30 random 20x fields per condition and normalizing to the mean cell surface area using ImageJ (NIH, Bethesda, MD) <sup>10</sup>.

### **Immunoblotting**

Following serum starvation, NRK49F or HT29 cells were incubated with N-Slit2 (30 nmol/l) for 10 min, then with TGF- $\beta$  for 30 min. In some experiments, cells were additionally pre-treated with the TBRI inhibitor SB431542 (Sigma-Aldrich, Oakville, ON, Canada) <sup>11</sup>. Cell lysates and/or tissue homogenates were prepared and separated by SDS-PAGE. Following transfer, membranes were incubated with Ab directed to phospho-Smad2 and to Smad2/3 (Cell Signaling, Danvers, MA), or to Robo-1 (Rockland Immunochemicals, Limerick, PA). The basal expression of TBRI and TBRII was similarly examined using Ab (Santa Cruz Biotechnology, Dallas, TX) directed to each of these proteins. Primary Ab were detected with HRP-conjugated goat anti-rabbit secondary antibody (Jackson ImmunoResearch). Quantitative analysis was performed by measuring band intensity using ImageJ (NIH). Smad2 phosphorylation was calculated as the ratio of band intensities for phospho-Smad2 to total Smad2 <sup>8</sup>.

### **Transfection and luciferase reporter assay**

NRK49F cells were serum starved overnight in DMEM containing 1% FBS, and then transfected with a Firefly luciferase reporter cDNA driven by tandem Smad-binding element (SBE) consensus motifs (a kind gift from Dr. A. Kapus), along with a control

Renilla luciferase vector constitutively driven by the HSV-thymidine kinase promoter (Promega, Madison, WI). After 16 h, cells were incubated with either N-Slit2 (30 nmol/L) or C-Slit2 (30 nmol/L) for 30 min, followed by stimulation with TGF- $\beta$  (10 ng/mL) and both Firefly and Renilla luminescence read 24 h later using a *Dual-Glo*<sup>®</sup> *Luciferase* kit and luminometer (Promega). Smad transcriptional activity was calculated as the Firefly:Renilla luminescence ratio <sup>12</sup>. Alternately, the same experiments were performed but instead NRK49F cells were first stimulated with TGF- $\beta$ , followed 4 h later by N-Slit2. In these experiments, luminescence was read 24 h after TGF- $\beta$  stimulation.

### **Unilateral ureteral obstruction mouse model**

Male C57BL/6 mice (6 – 8 weeks old) were purchased from Jackson Laboratory (Bar Harbor, ME), and underwent either left-sided unilateral ureteral obstruction (UUO, n = 42) or sham surgery (n = 12). Briefly, a left-sided flank incision was made in anesthetized mice, and the left kidney and ureter identified. The left ureter was then obstructed with two 4-0 silk suture ties just distal to the renal pelvis. Mice undergoing UUO surgery were randomized to receive injections of normal saline control vehicle (n = 18), N-Slit2 (2  $\mu$ g, n = 12), or a molar equivalent amount of C-Slit2 (0.4  $\mu$ g, n = 12). The first injection was administered intravenously (i.v.) 1 h prior to surgery, while a second injection was given intra-peritoneally (i.p.) 3 d later. Seven days after surgery, mice were sacrificed, and the left kidneys resected. Paraffin-embedded kidney sections were analyzed as described below for the renal ischemia-reperfusion injury experiments.

### **Murine kidney ischemia-reperfusion injury experiments**

Male C57BL/6 mice (age 6 – 8 wks old) underwent left-sided unilateral ischemia-reperfusion injury surgery as previously described<sup>1,13-15</sup>. During the entire procedure, the core temperature of the mice was maintained between 34 and 36°C with a heating pad. Following induction of anesthesia with inhaled 2% isoflurane, a left-sided flank incision was made, followed by exposure of the pedicle of the left kidney. Hilar vessels were cross-clamped for 45 min. Clamps were then removed, allowing the left kidney to reperfuse. Ambient post-operative air temperature was maintained between 30 – 32°C until mice had fully recovered.

#### *Study 1: Early Slit2 Treatment*

Mice undergoing ischemia-reperfusion injury surgery were randomized pre-operatively to receive injections of normal saline (n = 17), N-Slit2 (n = 17), or C-Slit2 (n = 7). The first injection was performed i.v. 1 h prior to induction of IRI, while subsequent injections were administered i.p. thrice weekly for the duration of the 14 d study. Sham-operated C57BL/6 mice (n = 6) served as healthy controls. Thirteen days after surgery, mice underwent nephrectomy of the uninjured right kidney. One day following this nephrectomy, blood was collected by cardiac puncture, and plasma urea and creatinine were measured using urease-spectrophotometric and picric acid-based assays respectively, as per the manufacturers' protocols<sup>1</sup>. Mice were sacrificed and the injured kidney resected.

At study end, the left kidneys of all mice were retrieved, and samples of each kidney were immersion fixed in 10% neutral buffered formalin. Formalin-fixed tissues were

embedded in paraffin and sectioned before staining with picosirius red, Masson's Trichrome, hematoxylin and eosin, Periodic Acid-Schiff, or an antibody directed to  $\alpha$ -smooth muscle actin (Dako, Burlington, Canada). Slides were digitally scanned at room temperature with an Aperio Scanscope XT scanner (Leica Biosystems) and whole kidney staining (excluding the renal pelvis) analyzed using Aperio Imagescope software as previously described<sup>8,9</sup>.

### *Study 2: Delayed Slit2 Treatment*

In separate experiments, mice undergoing ischemia-reperfusion injury surgery were randomized post-operatively to receive injections of normal saline (n = 15), N-Slit2 (n = 15) or C-Slit2 (n = 14). The first injection was administered i.p. 72 h after induction of IRI, while subsequent injections were given i.p. thrice weekly for the duration of the 14 d study. Sham-operated C57BL/6 mice (n = 3) served as healthy controls. Nephrectomy of the uninjured right kidney was performed 13 d after the initial surgery, and blood and kidneys were collected the next day as described in Study 1. Renal histological analysis was also performed as described in Study 1.

### **Quantitative real time PCR**

RNA was isolated from snap frozen mouse kidney tissue, reverse transcribed, and quantitative real time PCR was performed using SYBR green on an ABI Prism 7900HT Fast PCR System (Applied Biosystems, Foster City, CA). Primer sequences (ACGT Corp., Toronto, ON, Canada) were as follows: (1) ACTA2 forward: GAGTCCAGCACAAATACCAGTT, ACTA2 reverse: CACTGAACCCTAAGGCCAAC;

(2) COL3A1 forward: CATTGCGTCCATCAAAGCC, COL3A1 reverse: GAAAGGATGGAGAGTCAGGAA; (3) PAI1 forward: CGTGTCAGCTCGTCTACAG, PAI1 reverse: CTATGGTGAAACAGGTGGACT; and (4) GAPDH forward: GTGGAGTCATACTGGAACATGTAG, GAPDH reverse: AATGGTGAAGGTCGGTGTG. Experiments were performed in triplicate and data analysis was performed using the Applied Biosystems Comparative CT method.

### **Detection of Robo-1 in fibroblasts *in vivo***

Cryosections of the injured kidney from mice sacrificed 14 d following unilateral ureteral obstruction or sham surgery were stained with antibodies directed against Robo-1 (Rockland Immunochemicals) and  $\alpha$ -smooth muscle actin (Dako). The  $\alpha$ -smooth muscle actin antibody was directly conjugated to FITC. The primary Robo-1 antibody was detected with an Alexa 549-conjugated donkey anti-rabbit secondary antibody (Jackson ImmunoResearch). Cryosections were counter-stained with wheat germ agglutinin to identify cell membranes and imaged at room temperature using the Volocity imaging package (PerkinElmer) on a spinning disc DMIRE2 confocal microscope (Leica Microsystems) equipped with a Hamamatsu digital camera.

### **Statistical analysis**

A minimum of  $n = 3$  independent experiments was performed for all *in vitro* studies. All data are shown as mean  $\pm$  SEM unless otherwise stated. Graphpad Prism (version 5.0, GraphPad Software, San Diego, CA) was used to analyze the data. Data were analyzed

using a 1-way ANOVA with post-hoc Fisher's least significant difference analysis as appropriate.  $p < 0.05$  was deemed significant.

### **Study approval**

All animal experiments were approved by The Hospital for Sick Children Animal Care and Use Committee, and adhered to the NIH Guide for the Care and Use of Laboratory Animals.

## SUPPLEMENTAL REFERENCES

1. Chaturvedi, S, Yuen, DA, Bajwa, A, Huang, YW, Sokollik, C, Huang, L, Lam, GY, Tole, S, Liu, GY, Pan, J, Chan, L, Sokolskyy, Y, Puthia, M, Godaly, G, John, R, Wang, C, Lee, WL, Brumell, JH, Okusa, MD & Robinson, LA: Slit2 prevents neutrophil recruitment and renal ischemia-reperfusion injury. *J Am Soc Nephrol* 24: 1274-1287, 2013.
2. Tole, S, Mukovozov, IM, Huang, YW, Magalhaes, MA, Yan, M, Crow, MR, Liu, GY, Sun, CX, Durocher, Y, Glogauer, M & Robinson, LA: The axonal repellent, Slit2, inhibits directional migration of circulating neutrophils. *J Leukoc Biol* 86: 1403-1415, 2009.
3. Patel, S, Huang, YW, Reheman, A, Pluthero, FG, Chaturvedi, S, Mukovozov, IM, Tole, S, Liu, GY, Li, L, Durocher, Y, Ni, H, Kahr, WH & Robinson, LA: The cell motility modulator Slit2 is a potent inhibitor of platelet function. *Circulation* 126: 1385-1395, 2012.
4. Zhou, WJ, Geng, ZH, Chi, S, Zhang, W, Niu, XF, Lan, SJ, Ma, L, Yang, X, Wang, LJ, Ding, YQ & Geng, JG: Slit-Robo signaling induces malignant transformation through Hakai-mediated E-cadherin degradation during colorectal epithelial cell carcinogenesis. *Cell Res* 21: 609-626, 2011.
5. Wu, JY, Feng, L, Park, HT, Havlioglu, N, Wen, L, Tang, H, Bacon, KB, Jiang, Z, Zhang, X & Rao, Y: The neuronal repellent Slit inhibits leukocyte chemotaxis induced by chemotactic factors. *Nature* 410: 948-952, 2001.

6. Ku, CH, Johnson, PH, Batten, P, Sarathchandra, P, Chambers, RC, Taylor, PM, Yacoub, MH & Chester, AH: Collagen synthesis by mesenchymal stem cells and aortic valve interstitial cells in response to mechanical stretch. *Cardiovascular Research* 71: 548-556, 2006.
7. Rhaleb, NE, Peng, H, Harding, P, Tayeh, M, LaPointe, MC & Carretero, OA: Effect of N-acetyl-seryl-aspartyl-lysyl-proline on DNA and collagen synthesis in rat cardiac fibroblasts. *Hypertension* 37: 827-832, 2001.
8. Yuen, DA, Connelly, KA, Advani, A, Liao, C, Kuliszewski, MA, Trogadis, J, Thai, K, Advani, SL, Zhang, Y, Kelly, DJ, Leong-Poi, H, Keating, A, Marsden, PA, Stewart, DJ & Gilbert, RE: Culture-modified bone marrow cells attenuate cardiac and renal injury in a chronic kidney disease rat model via a novel antifibrotic mechanism. *PLoS One* 5: e9543, 2010.
9. Yuen, DA, Connelly, KA, Zhang, Y, Advani, SL, Thai, K, Kabir, G, Kepecs, D, Spring, C, Smith, C, Batruch, I, Kosanam, H, Advani, A, Diamandis, E, Marsden, PA & Gilbert, RE: Early outgrowth cells release soluble endocrine antifibrotic factors that reduce progressive organ fibrosis. *Stem Cells* 31: 2408-2419, 2013.
10. Hotulainen, P & Lappalainen, P: Stress fibers are generated by two distinct actin assembly mechanisms in motile cells. *J Cell Biol* 173: 383-394, 2006.
11. Gaedeke, J, Noble, NA & Border, WA: Curcumin blocks multiple sites of the TGF-beta signaling cascade in renal cells. *Kidney Int* 66: 112-120, 2004.
12. Masszi, A, Speight, P, Charbonney, E, Lodyga, M, Nakano, H, Szaszi, K & Kapus, A: Fate-determining mechanisms in epithelial-myofibroblast transition: major inhibitory role for Smad3. *J Cell Biol* 188: 383-399, 2010.

13. Furuichi, K, Gao, JL & Murphy, PM: Chemokine receptor CX3CR1 regulates renal interstitial fibrosis after ischemia-reperfusion injury. *Am J Pathol* 169: 372-387, 2006.
14. Jang, HR, Gandolfo, MT, Ko, GJ, Satpute, SR, Racusen, L & Rabb, H: B cells limit repair after ischemic acute kidney injury. *J Am Soc Nephrol* 21: 654-665, 2010.
15. Thorenz, A, Chen, R, Huper, K, Hensen, B, Klemann, C, Meier, M, Klos, A & Guler, F: Complement Receptor C5L2 Improves Renal Perfusion Impairment after Ischemia Reperfusion Injury. *FASEB J* 29, 2015.